Received: 12 July 2022 | Accepted: 10 October 2022

DOI: 10.1111/1751-7915.14162

RESEARCH ARTICLE

microbial biotechnology Open Access

Enhancing tellurite and selenite bioconversions by overexpressing a methyltransferase from *Aromatoleum* sp. CIB

Elena Alonso-Fernandes[1] | **Helga Fernández-Llamosas**[1] | **Irene Cano**[1] | **Cristina Serrano-Pelejero**[1] | **Laura Castro**[2] | **Eduardo Díaz**[1] | **Manuel Carmona**[1]

[1]Microbial and Plant Biotechnology Department, Centro de Investigaciones Biológicas Margarita Salas-CSIC, Madrid, Spain

[2]Department of Material Science and Metallurgical Engineering, Facultad de Químicas, Universidad Complutense de Madrid, Madrid, Spain

Correspondence
Manuel Carmona, Microbial and Plant Biotechnology Department, Centro de Investigaciones Biológicas Margarita Salas-CSIC, Ramiro de Maeztu 9, 28040 Madrid, Spain.
Email: mcarmona@cib.csic.es

Funding information
Consejo Superior de Investigaciones Científicas, Grant/Award Number: CSIC 2019 20E005; European Union H2020, Grant/Award Number: 101000733; Ministerio de Ciencia e Innovación, Grant/Award Number: BIO2016-79736-R, PCI2019-111833-2 and PID2019-110612RB-I00

Abstract

Pollution by metalloids, e.g., tellurite and selenite, is of serious environmental concern and, therefore, there is an increasing interest in searching for ecologically friendly solutions for their elimination. Some microorganisms are able to reduce toxic tellurite/selenite into less toxic elemental tellurium (Te) and selenium (Se). Here, we describe the use of the environmentally relevant β-proteobacterium *Aromatoleum* sp. CIB as a platform for tellurite elimination. *Aromatoleum* sp. CIB was shown to tolerate 0.2 and 0.5 mM tellurite at aerobic and anaerobic conditions, respectively. Furthermore, the CIB strain was able to reduce tellurite into elemental Te producing rod-shaped Te nanoparticles (TeNPs) of around 200 nm length. A search in the genome of *Aromatoleum* sp. CIB revealed the presence of a gene, *AzCIB_0135*, which encodes a new methyltransferase that methylates tellurite and also selenite. *AzCIB_0135* orthologs are widely distributed in bacterial genomes. The overexpression of the *AzCIB_0135* gene both in *Escherichia coli* and *Aromatoleum* sp. CIB speeds up tellurite and selenite removal, and it enhances the production of rod-shaped TeNPs and spherical Se nanoparticles (SeNPs), respectively. Thus, the overexpression of a methylase becomes a new genetic strategy to optimize bacterial catalysts for tellurite/selenite bioremediation and for the programmed biosynthesis of metallic nanoparticles of biotechnological interest.

INTRODUCTION

The interest for metalloids, e.g., tellurium (Te) and selenium (Se), has increased exponentially in the last years due to their industrial utility, particularly in technological disposals such as photovoltaic panels, rechargeable batteries, or biomedicine devices (Ba et al., 2010; Johnson et al., 1999; Turner et al., 2012; Zannoni et al., 2008) and also on cosmetics, packing, coating, or biotechnology (Thakkar et al., 2010). Such an increase in the demand for metalloids has raised the concern about potential environmental and human health

issues (Chasteen et al., 2009; Roy & Hardej, 2011; Shie & Deeds, 1920; Taylor, 1996; Vij & Hardej, 2012; Widy-Tyszkiewicz et al., 2002; Wiklund et al., 2018; Wu et al., 2014). For example, while elemental tellurium [Te (0)] is not very toxic, tellurite [Te (IV)] displays strong oxidizing properties and can displace Se from the selenoproteins altering a high number of cellular functions (Ba et al., 2010; Turner et al., 1998). Although selenite [Se (IV)] is less toxic than tellurite, its release into the environment may lead to a strong negative impact especially in aquatic ecosystems (Morlon et al., 2005). Te and Se can also be part of methylated volatile compounds, such as methyltellurides and methylselenides, which are easily detected by their strong garlic acid smell (Ranjard et al., 2002, 2003; Zannoni et al., 2008).

Most bacteria are sensitive to tellurite concentrations as low as 10 μM, which is about 100 times lower than that of other toxic elements, such as copper, chromium, iron, or cadmium (Chasteen et al., 2009; Taylor, 1999). Nevertheless, some bacteria have developed mechanisms of resistance to tellurite. Although most of the molecular mechanisms of resistance remain unknown, there have been described some gene clusters associated with specific tellurite resistance (Chasteen et al., 2009; Presentato et al., 2019), such as the *kilA* operon (*klaAklaBtelB*) from the plasmid RK2 (Walter et al., 1991), the *tehAB* operon that was first identified in *Escherichia coli* K12 strains (Taylor et al., 1994) or the well-studied *terABCDEF* cluster of *E. coli* O157:H7 (Taylor et al., 2002). Moreover, it is important to remark the relevance of some thiopurine *S*-methyltransferases (TPMT) in tellurite resistance (Honchel et al., 1993; Prigent-Combaret et al., 2012). The TPMT proteins are cytoplasmatic enzymes that catalyse the *S*-adenosylmethionine (SAM)-dependent transmethylation of thiopurines rendering thiopurine S-methylethers (Honchel et al., 1993). It has been demonstrated that this enzyme might also use the SAM molecule to catalyse the methylation of Te into dimethyl telluride and/or dimethyl ditelluride (Bonificio & Clarke, 2014; Honchel et al., 1993; Ollivier et al., 2011). In fact, well-studied TPMT from *Pseudomonas syringae* is able to methylate Te into volatile dimethyl telluride and dimethyl ditelluride (Prigent-Combaret et al., 2012). Bacteria have also developed mechanisms of resistance to selenite, some of which involve the participation of uncharacterized energy-dependent transporters (Fernández-Llamosas et al., 2016), or the methylation of inorganic and organic Se compounds into volatile dimethyl selenides and dimethyl diselenides by TPMT enzymes (Moreno-Martin et al., 2021; Ranjard et al., 2002; Ruiz-Fresneda et al., 2020).

Many tellurite and selenite resistant bacteria use the reduction of these metalloids to elemental and insoluble Te (0) or Se (0) as another mechanism of resistance, since these metallic forms are much less toxic (Chasteen et al., 2009). Although the molecular mechanisms underlying metalloid reduction are not fully understood, they might involve the participation of thiol-containing proteins, glutathione reductases (Turner et al., 2012), nitrate/nitrite reductases (Sabaty et al., 2001), and a vast variation of small molecules and enzymatic activities, in different bacterial species (Basaglia et al., 2007; Chen & Strous, 2013; Debieux et al., 2011; Kessi & Hanselmann, 2004).

Interestingly, some bacteria are able to couple the reduction of tellurite to Te (0) and/or selenite to Se (0) for the production of Te nanoparticles (TeNPs) and/or Se nanoparticles (SeNPs), which can accumulate intracellularly, either in the cytoplasm or in the periplasm (Baesman et al., 2009; Fernández-Llamosas et al., 2016, 2017; Ramos-Ruiz et al., 2016), or extracellularly (Borghese et al., 2016; Ramos-Ruiz et al., 2016; Turner et al., 2012; Zare et al., 2012). TeNPs have practical applications such as the construction of nanowires (Chou et al., 2016; Presentato et al., 2018). In addition, TeNPs display optoelectronic and semiconducting properties that allow them to be used in microelectronic circuits or solar cells (Presentato et al., 2018). The use of bacteria as biocatalysts is an attractive, economical, and green alternative to large scale synthesis of metallic NPs. Whereas physicochemical synthesis of metallic NPs has strong safety and environmental concerns since it requires high temperatures and pressures, with risk of explosions or spill events (Presentato et al., 2019), biological methods offer efficient, economic, and sustainable methods of production of metallic NPs homogeneous in size and with high thermodynamic stability. Understanding the molecular mechanisms underlying the bacterial production of metalloids nanostructures is gaining increased interest in the field of nanotechnology, with the potential for exploitation in bionanomaterial fabrication (Butler et al., 2012).

Aromatoleum sp. CIB (formerly *Azoarcus* sp. CIB) is a denitrifying β-Proteobacterium that has been considered as a model system to study several environmental traits (Martín-Moldes et al., 2015). Thus, the strain CIB is capable to degrade under aerobic and/or anaerobic conditions a high number of aromatic compounds, including some toxic hydrocarbons such as toluene and *m*-xylene (Blázquez et al., 2018; Carmona et al., 2009; Juárez et al., 2013; López-Barragán et al., 2004). The CIB strain is also able to colonize rice roots as endophyte and preserve the plants from environmental stress (Fernández-Llamosas et al., 2014, 2020). Furthermore, *Aromatoleum* sp. CIB resists a good number of metals and metalloids including zinc, nickel, cadmium (Martín-Moldes et al., 2015), selenite (Fernández-Llamosas et al., 2016), arsenite, and arsenate (Durante-Rodríguez et al., 2019) and produce Se nanoparticles (Fernández-Llamosas et al., 2016). In this work, we have demonstrated that *Aromatoleum* sp. CIB shows tellurite resistance, and we have identified the *AzCIB_0135* gene encoding a new methyltransferase

that methylates tellurite and also selenite. The overexpression of the *AzCIB_0135* gene both in *E. coli* and *Aromatoleum* sp. CIB speeds up tellurite and selenite removal, and it enhances the production of TeNPs and SeNPs, respectively, hence revealing a new genetic strategy to optimize bacterial catalysts for the biosynthesis of such metallic nanoparticles that are of major industrial interest.

EXPERIMENTAL PROCEDURES

Bacterial strains, plasmids and growth conditions

Bacterial strains and plasmids used in this work are detailed in Table 1. *Aromatoleum* sp. CIB (previously termed *Azoarcus* sp. strain CIB) was deposited in the Spanish Type Culture Collection (CECT #5669). *Aromatoleum* cells were grown on MC medium (MA basal medium plus trace elements and vitamins). MA basal medium is composed of the following, per litre of distillated water: (0.33 g of KH_2PO_4, 1.2 g of Na_2HPO_4, 0.11 g of NH_4Cl, 0.1 g $MgSO_4 \times 7H_2O$, 0.04 g of $CaCl_2$ [pH 7.5]) supplemented with trace elements (stock solution 100×; 1.5 g of nitrilotriacetic acid, 3 g of $MgSO_4 \times 7H_2O$, 0.5 g of $MnSO_4 \times 2H_2O$, 1 g of NaCl, 0.1 g of $FeSO_4 \times 7H_2O$, 0.18 g of $CoSO_4 \times 7H_2O$, 0.1 g of $CaCl_2 \times 2H_2O$, 0.18 g of $ZnSO_4 \times 7H_2O$, 0.01 g of $CuSO_4 \times 5H_2O$, 0.02 g of $KAl(SO_4)_2 \times 12H_2O$, 0.01 g of H_3BO_3, 0.01 g of $Na_2MoO \times 2H_2O$, 0.025 g of $NiCl_2 \times 6H_2O$ and 0.3 mg of $Na_2SeO_3 \times 5H_2O$ [pH 6.5] per litre of deionized water), vitamin solution (stock 1000×; 20 mg of biotin, 20 mg of folic acid, 10 mg of pyridoxine-HCl, 50 mg of thiamine-$HCl \times 2H_2O$, 50 mg of riboflavin, 50 mg of nicotinic acid, 50 mg of calcium D-pantothenic acid, 50 mg of vitamin B12, and 50 mg of *p*-aminobenzoic acid per litre of distilled water; López-Barragán et al., 2004). For anaerobic growth, 15 ml of MC medium was flushed with N_2, and the bottles were sealed with rubber stoppers and aluminium crimp seals before being autoclaved, and 10 mM potassium nitrate was added as electron acceptor (López-Barragán et al., 2004). As carbon source, 0.2% (w/v) pyruvate was added. For anaerobic growth conditions, the carbon source and the bacterial inoculum were injected through the stopper with a syringe. All the cultures were incubated at 30°C. *E. coli* strains were grown in lysogeny broth (LB) medium (Miller, 1972) at 37°C. When required, gentamicin was added at 10 $\mu g\,ml^{-1}$. Growth was monitored by measuring the absorbance at 600 nm (A_{600}).

The microbial growth and reduction of tellurite/selenite was studied in *Aromatoleum* sp. CIB and *E. coli* DH10B cells cultured aerobically or anaerobically in MC medium with pyruvate 0.2% (w/v) or LB, respectively, supplemented with the concentrations of potassium tellurite or sodium selenite indicated in each experiment. *E. coli* DH10B was selected because it displays high tellurite sensitivity. The change in colour of the cultures was monitored along the growth.

TABLE 1 Bacterial strains and plasmids used in this study

Strain or plasmid	Relevant genotype and characteristic(s)	Reference or source
E. coli strains		
DH10B	F$^-$ Δ(*ara-leu*)*7697*[Δ(*rapA*'-*cra*')] Δ(*lac*)*X74*[Δ('*yahH-mhpE*)] *galK16 galE15* φ80d*lacZΔM15 recA1 relA1 endA1* Tn*10.10 nupG rpsL150*(Str^r) *rph*$^+$ *spoT1* λ$^-$	Casadaban and Cohen (1980)
DH10B (pIZ2)	Gm^r, DH10B strain carrying the pIZ2 plasmid	This work
DH10B (pIZ2-0135)	Gm^r, DH10B strain carrying the pIZ2-0135 plasmid	This work
DH10B (pIZ2-TPMTPS)	Gm^r, DH10B strain carrying the pIZ2-TPMTPS plasmid	This work
S17-1λ*pir*	Tp^r Sm^r *recA thi hsdRM*$^+$ RP4::2-Tc::Mu::Km λ*pir* phage lysogen	De Lorenzo and Timmis (1994)
Aromatoleum strains		
CIB	Wild type strain	López-Barragán et al. (2004)
CIB (pIZ2)	Gm^r, CIB strain carrying the pIZ2 plasmid	This work
CIB (pIZ2-0135)	Gm^r, CIB strain carrying the pIZ-0135 plasmid	This work
Plasmids		
pIZ1016	Gm^r, pBBR1MCS-5 derivative harbouring the *Ptac* promoter and the *lacI* gene from pMM40	Moreno-Ruiz et al. (2003)
pIZ2	Gm^r, extended pIZ1016 polylinker. EcoRI, ClaI, SpeI, XvaI, SalI, PstI (SbfI), SphI, HindIII and SacI.	Acedos et al. (2021)
pIZ2-0135	Gm^r, 684 bp AzCIB_0135 cloned in double-digested EcoRI/HindIII pIZ2 plasmid	This work
pIZ2-TPMTPS	Gm^r, 657 bp *P. syringae* synthetic *tpmt* gene cloned in double-digested XbaI/HindIII pIZ2 plasmid	This work

Serial dilutions of the cultures were plated on solid MC medium with 0.2% pyruvate, and colony forming units (CFU) were counted after 48 h of incubation at 30°C.

Molecular biology techniques

Standard molecular biology techniques were performed as previously described (Sambrook & Rusell, 2001). DNA fragments were purified with Gene-Turbo (BIO101 Systems). Plasmids and PCR products were purified with a High Pure Plasmid and PCR Product Purifications kits (Roche), respectively. Oligonucleotides were supplied by Sigma Co., and they were used for the construction of the pIZ2-0135 plasmid. The oligonucleotides sequences for amplification of the *AzCIB_0135* gene from the CIB genome and its further cloning into the pIZ2-0135 plasmid are: 5′AzCIB_0135: 5′-ATATATGAATTCTGACCTAAGGAGGTAAATAATGGACGCCAACTTCTG-3′ (a restriction EcoRI site underlined) and 3′AzCIB_0135: 5′- ATATATAAGCTTTCAGTCCTTCCTCAGCAGCC-3′ (a restriction HindIII site underlined). A synthetic optimized codon usage sequence for *E. coli* of the *tpmt* gene from *P. syringae* designed using the Geneious program was supplied by GenScript® (Figure S1) cloned in the pIZ2 plasmid, as plasmid pIZ2-TPMTPS. All cloned inserts and DNA fragments were confirmed by DNA sequencing with fluorescently labelled dideoxynucleotide terminators (Sanger et al., 1977) and AmpliTaq FS DNA polymerase (Applied Biosystems) in an ABI Prism 377 automated DNA sequencer (Applied Biosystems). Transformations of *E. coli* cells was carried out by using the RbCl method or by electroporation (Gene Pulser, Bio-Rad) (Sambrook & Rusell, 2001). Plasmids were transferred from *E. coli* S17-1λpir (donor strain) to *Aromatoleum* sp. CIB (recipient strain) by biparental filter mating (De Lorenzo & Timmis, 1994), and exconjugants strains *Aromatoleum* sp. CIB (pIZ2) and *Aromatoleum* sp. CIB (pIZ2-0135) were isolated aerobically on gentamicin-containing MC agar plates harbouring 10 mM glutarate as the sole carbon source for counter selection of donor cells.

Characterization of TeNPs and SeNPs

For field emission Scanning Electron Microscopy (SEM), the samples were filtered through 0.2 μm pore-size filters and successively dehydrated with acetone/water mixtures of 30, 50 and 70% acetone, respectively, and stored overnight at 4°C in 90% acetone. After critical-point drying, samples were coated with graphite and gold and examined with a JEOL JSM-6330F microscope. For Transmission Electron Microscopy (TEM) analysis, the samples were prepared by placing drops of the cell culture onto carbon-coated copper grids and allowing the solvent to evaporate. TEM observations were performed on a JEOL model JEM-2100 instrument operated at an accelerating voltage of 200 kV. The chemical composition of the TeNPs observed was determined by Energy-Dispersive X-ray spectroscopy (EDX) as previously described (Li et al., 2014). Size of metallic nanoparticles was determined by using the Image J software (Collins, 2007).

TeNPs purification

For the purification of the TeNPs, a previously published protocol was followed (Bahrami et al., 2012). This protocol is based on a separation by centrifugation of the TeNPs produced by the bacteria in a mixture composed by chloroform, ethyl alcohol, and water (3:1:4).

Determination of the Te (0) and Se (0) produced and tellurite and selenite determination

To evaluate the production of Te (0) and Se (0), 9 ml of cells cultured in the presence of tellurite or selenite, respectively, were collected along the growth curve. Cells were centrifuged 20 min at 1800 ***g***, pellets were washed twice with saline solution and resuspended in 500 μl distilled water, and the cells were lysed by sonication. The solution was immediately filtered using MCE membrane filters of 0.025 μm (Millipore). The filter was rinsed in 9 ml H_2O_2 30% until complete oxidation and dissolution of the metalloids deposited (4 h). Tellurite and selenite concentrations were determined by inductively coupled plasma optical emission spectrometry (ICP-OES; Perkin Elmer Optima 2100 DV; Nawaz et al., 2015).

Sequence data analyses

Nucleotide sequence analyses were done at the National Center for Biotechnology Information (NCBI) server. Pairwise and multiple protein sequence alignments were made with the ClustalW program (Thompson et al., 1994) at the EMBL-EBI server. Phylogenetic analysis was carried out according to the Kimura two-parameter method (Kimura, 1980), and a tree was reconstructed using the neighbour-joining method (Saitou & Nei, 1987) of the PHYLIP program (Felsenstein, 1993).

3D-modelling of AzCIB_0135 protein

The three-dimensional model of AzCIB_0135 was generated by using the Alphafold program (Jumper et al., 2021), and it was visualized with the PyMol program (http://pymol.sourceforge.net/).

RESULTS AND DISCUSSION

Tellurite resistance of *Aromatoleum* sp. CIB

To expand our knowledge about the abilities of *Aromatoleum* sp. CIB in metal bioremediation, we analysed the level of resistance of the strain CIB to the metalloid tellurite. The sensibility of the strain CIB was tested by growing cells, aerobically or anaerobically, in the presence of tellurite at concentrations ranging from 0 to 1 mM. Whereas in aerobic conditions cells were able to grow in the presence of up to 0.2 mM, tellurite (Figure 1A), under anaerobic conditions cells grew up to 0.5 mM tellurite, although a decrease of around one order of magnitude in colony forming units was observed. (Figure 1B). In both cases, tellurite induced cellular death during the first 24 h of incubation as detected by the decrease in the number of viable cells (Figure 1). This phenomenum has been already described in other microorganisms (Borghese et al., 2004), suggesting that tellurite causes serious metabolic damages, most likely at the membrane level (Kessi et al., 2022) and by inactivating thiolic groups of cellular proteins (Muñoz-Díaz et al., 2022; Tucker et al., 1962; Zannoni et al., 2008). In fact, phase contrast microscopy showed that in the presence of tellurite the *Aromatoleum* sp., CIB cells were less mobile and often clustered in clots instead of being the highly motile individual cells that were observed in cultures grown in the absence of tellurite (Figure S2A,B). Electron microscopy showed that cells grown in the presence of tellurite were shorter and apparently with lower amounts of intracellular polyhydroxyalkanoates (PHA) granules (Figure S2C,D). This shorter size of the cells was also observed in SEM (Figure S2E,F). All these observations indicated that although the CIB strain was able to grow in the presence of tellurite, an important effect of this metalloid on cell morphology was detected, as previously reported in other bacteria such as *Rhodopseudomonas palustris* strain TX618 (Xie et al., 2018) or *Pseudomonas putida* KT2440 (Montenegro et al., 2020).

The kinetics of cell growth and tellurite removal was followed by cultivating *Aromatoleum* sp. CIB in the presence of 0.1 mM tellurite (Figure 2). Under aerobic conditions, around 40% of initial tellurite was removed in 10 days. However, under anaerobic conditions, up to 60% of initial tellurite was removed after 10 days (Figure 2). Interestingly, in both cases, the removal of tellurite was more efficient when the cells reached the stationary phase of growth (Figure 2).

Most bacteria are sensitive to very low concentrations of tellurite (in the micromolar range) (Avazéri et al., 1997; Moore & Kaplan, 1992; Taylor, 1996, 1999), and resistant bacteria usually show minimum inhibitory concentrations (MIC) of <2 mM (Borghese et al., 2004). Nevertheless, several bacterial strains have been reported to grow in the presence of higher tellurite concentrations (Table S1). Bacteria such as *Bacillus selenitireducens* (Baesman et al., 2007) or *Raoultella* sp. WYA (Nguyen et al., 2019) presented similar tellurite reduction rates than that observed in *Aromatoleum* sp. CIB; however, a good number of bacteria are able to reduce tellurite at higher speed, e.g., some strains of *Shewanella* (Valdivia-González et al., 2018) or *Pseudomonas pseudoalcaligenes* strain Te (Forootanfar et al., 2015). Although *Aromatoleum* sp. CIB cannot be considered as a hyperesistant strain that removes quickly tellurite (Table S1), it is able to tolerate significant concentrations of tellurite, specially under anaerobic conditions. These results are in agreement with the fact that tellurite acts as a strong oxidizer able to generate reactive oxygen species (ROS; Borsetti et al., 2005; Calderón et al., 2006; Pérez et al., 2007; Tantaleán et al., 2003; Tremaroli et al., 2007), and they suggest that strain CIB has evolved a mechanism(s) to bypass the lethal effect of tellurite that might be similar to any of those previously described in other bacteria (Baesman et al., 2009; Basaglia et al., 2007; Chen & Strous, 2013; Debieux et al., 2011; Kessi & Hanselmann, 2004; Prigent-Combaret et al., 2012; Turner et al., 2012).

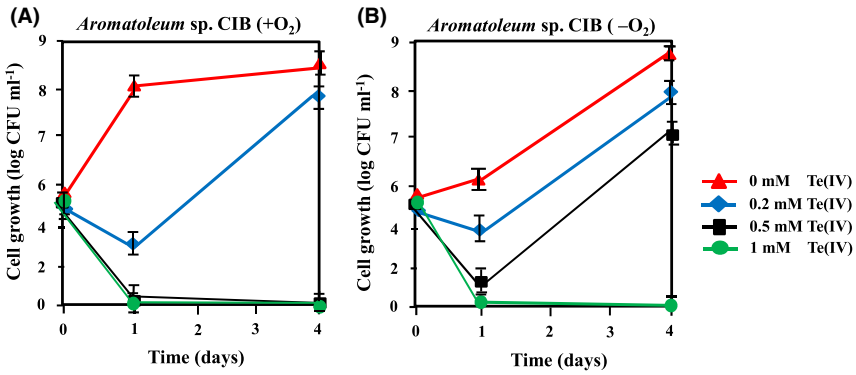

FIGURE 1 Time course of the growth of *Aromatoleum* sp. CIB in aerobic (A) or anaerobic (B) conditions in MC medium supplemented with pyruvate 0.2% (w/v) and tellurite at concentrations of 0 mM (red), 0.2 mM (blue), 0.5 mM (black), or 1 mM (green). The means of three independent experiments are represented and error bars show the standard deviation.

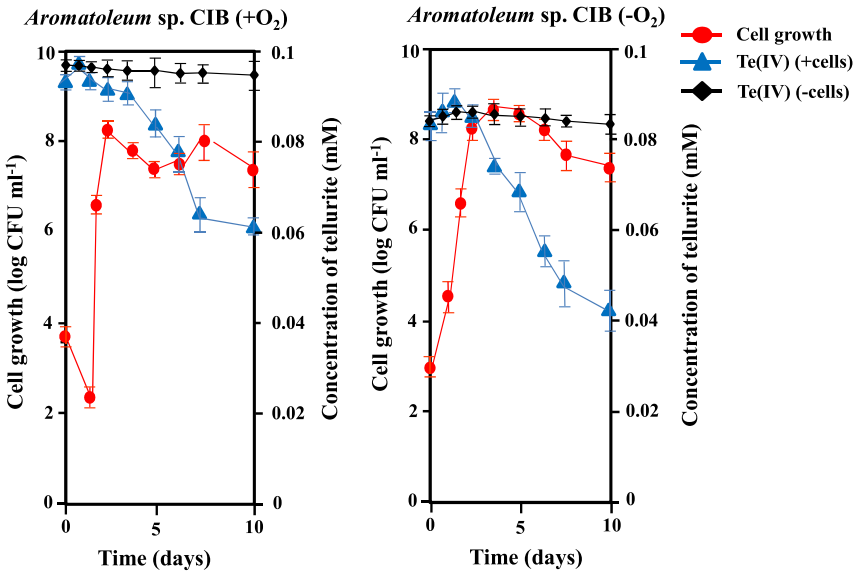

FIGURE 2 Time course of growth and tellurite removal by *Aromatoleum* sp. CIB. CIB cells were grown aerobically ($+O_2$) or anaerobically ($-O_2$) in MC medium supplemented with 0.2% pyruvate and containing 0.1 mM tellurite. Growth was measured as CFU ml^{-1} (red circles), and tellurite depletion (blue triangles) was determined by using ICP-OES as indicated in materials and methods. Tellurite concentration in the absence of bacteria is also indicated (black rhombs). Error bars represent standard deviation of the values of at least three independent experiments.

Bioproduction of Te nanoparticles by *Aromatoleum* sp. CIB

Most microorganisms able to tolerate tellurite share the ability to reduce this metalloid to the less toxic elemental Te, generating the characteristic black deposits (Chasteen et al., 2009; Tucker et al., 1962). *Aromatoleum* sp. CIB growing in medium containing 0.1 mM tellurite also produced black deposits (Figure S3) suggesting that tellurite removal was due to its reduction to insoluble black elemental Te. We then analysed whether the Te produced was deposited in form of nanoparticles (TeNPs). Bacteria were collected after 4 and 7 days of aerobic or anaerobic growth in the presence of tellurite, and they were observed by using TEM and SEM. TEM confirmed the presence of group of cylindrical electron-dense nanoparticles located inside the cells under both aerobic (Figure 3) and anaerobic (Figure 4) conditions. Rods presented sizes around 250 nm long in aerobic conditions, and 100 nm long in anaerobic conditions. The length of the TeNPs increased slightly in cells grown for longer incubation times (Figures 3 and 4), as it has been already reported in other bacterial cultures (Presentato et al., 2018). SEM preparations showed lysed cells with the rods adhered to the cell debris (Figure S4). TeNPs were purified, observed by TEM (Figure 5A), and analysed by EDX (Figure 5B). The rods were composed of metallic Te accompanied by oxygen, nitrogen, phosphorous, and sulfur (Figure 5B). The X-ray diffraction pattern indicates that tellurium crystalizes in the hexagonal lattice P3121 space group (JCPDS pattern 03-065-3370; inset Figure 5B). The production of crystalline TeNPs represents an advantage over the amorphous forms since they are more thermodynamically stable (Presentato et al., 2019), and their optical and electronic properties are useful for application in optic, thermo and electronic devices (Presentato et al., 2018). The peaks observed in EDX analysis corresponding to N, P, and S had been previously reported in EDX analyses of other bacterial TeNPs (Baesman et al., 2009) and could be correlated with the presence of an organic coating during the formation of the TeNPs that prevents their coalescence and, somehow, guides their final structure (Bulgarini et al., 2021; Piacenza, Presentato, & Turner, 2018; Piacenza, Presentato, Zonaro, et al., 2018). Although bacterial formation of spherical TeNPs has been described (Zonaro et al., 2015), most studies report the formation of intracellular (Baesman et al., 2007, 2009; Zare et al., 2012), periplasmic (Trutko et al., 2000) or extracellular (Borghese et al., 2016) stick-shaped TeNPs (Ramos-Ruiz et al., 2016; Zare et al., 2012), similar to those produced by *Aromatoleum* sp. CIB (Table S1) and also to those synthesized by chemical means (Kim & Park, 2012).

Many reports attributed the reduction of tellurite to an unspecific mechanism of resistance to this metalloid, as described in some strains of *E. coli*, *Rhodobacter sphaeroides*, *Staphylococcus aureus*, or *Pseudomonas aeruginosa* (Avazéri et al., 1997; Harrison et al., 2004; Summers & Jacoby, 1977). Some of the enzymes proposed to be involved on tellurite reduction, e.g., nitrate reductases, terminal oxidases, dehydrogenases, methyltransferases, etc. (Avazéri et al., 1997; Díaz-Vásquez et al., 2014; Sabaty et al., 2001; Trutko et al., 2000),

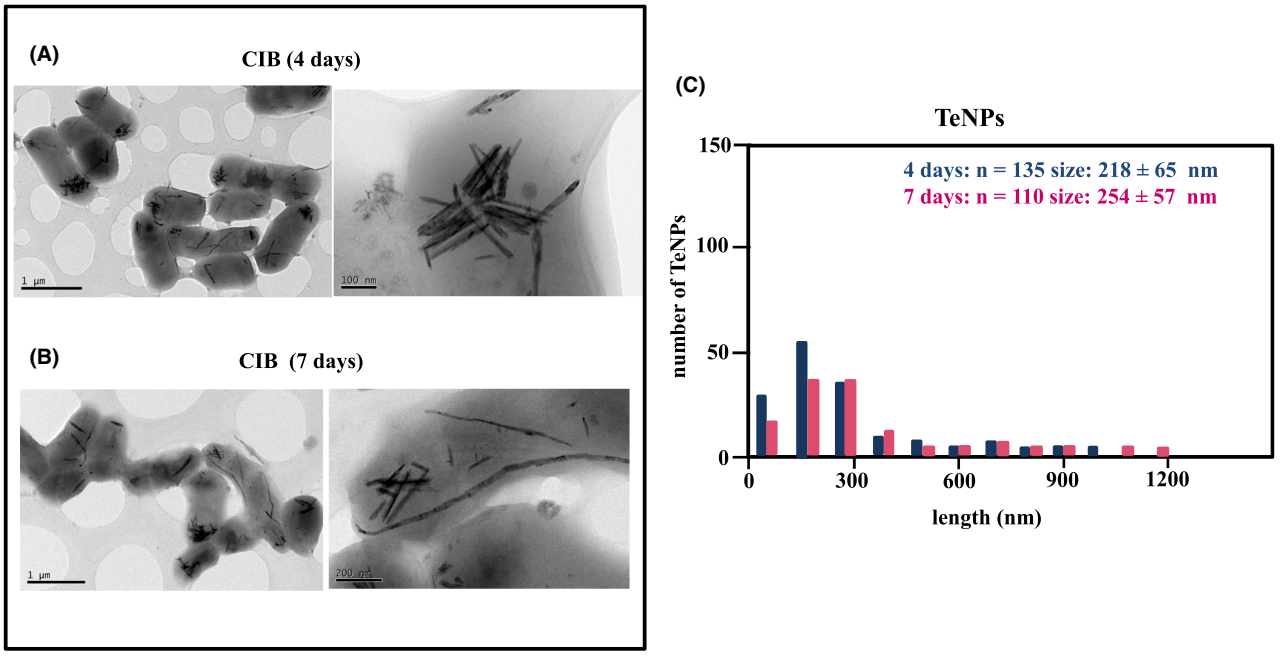

FIGURE 3 Microscopic observations and size distribution of Te nanoparticles (TeNPs) produced by *Aromatoleum* sp. CIB in aerobic conditions. TeNPs were produced by *Aromatoleum* sp. CIB grown aerobically in MC medium supplemented with 0.1 mM tellurite for 4 days (A) or 7 days (B). Transmission Electron Microscopy analysis shows nanoparticles inside the cells. Length distribution (in nm) of the TeNPs produced at 4 days (blue) and 7 days (red) is detailed in (C), where n represents the number of nanoparticles used for the size measurement.

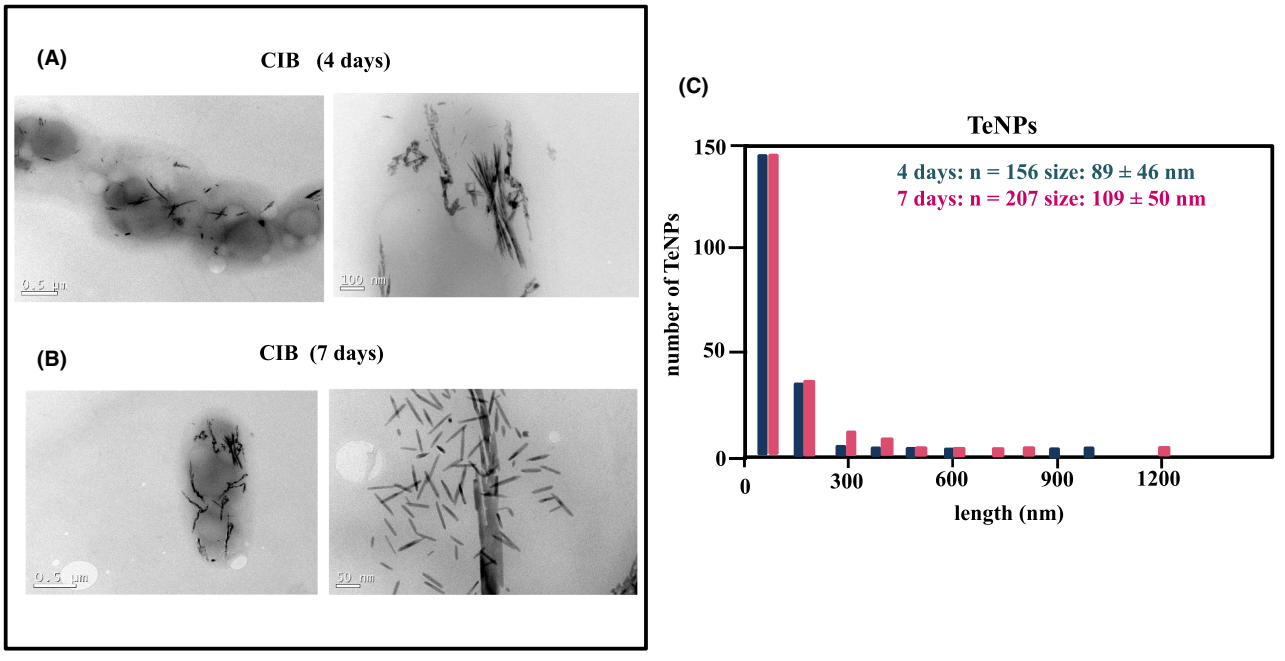

FIGURE 4 Microscopic observations and size distribution of Te nanoparticles (TeNPs) produced by *Aromatoleum* sp. CIB in anaerobic conditions. TeNPs were produced by *Aromatoleum* sp. CIB grown anaerobically in MC medium supplemented with 0.1 mM tellurite for 4 days (A) or 7 days (B). Transmission Electron Microscopy analysis shows nanoparticles inside the cells. Length distribution (in nm) of the TeNPs produced at 4 days (blue) and 7 days (red) is detailed in (C), where n represents the number of nanoparticles used for the size measurement.

are connected with bacterial metabolism and they are present in *Aromatoleum* sp. CIB (Martín-Moldes et al., 2015). A deeper study to elucidate the participation of these enzymes in tellurite reduction and TeNPs production in the CIB strain is underway.

The gene AzCIB_0135 from *Aromatoleum* sp. CIB encodes a tellurite methylase

The search of specific mechanisms involved in resistance to tellurite has a great interest since it has been

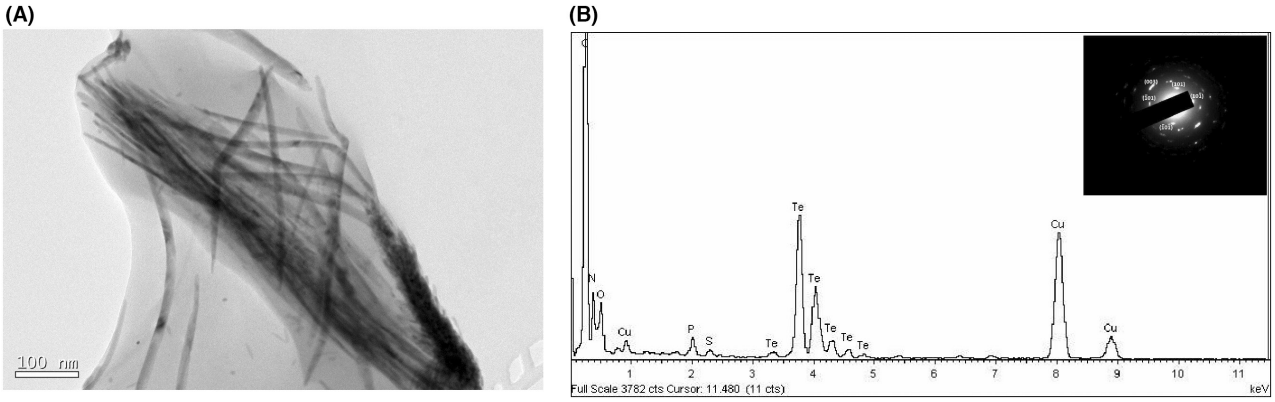

FIGURE 5 Microscopic observation and analysis of purified Te nanoparticles (TeNPs). (A) Transmission Electron Microscopy observation of the purified TeNPs produced by *Aromatoleum* sp. CIB showing their rod shape. (B) Energy-Dispersive X-ray spectroscopy analysis of one TeNP of panel (A). In the inset are shown the diffuse rings in the SAED (selected area electron diffraction) pattern of one TeNP.

observed that increasing the resistance to tellurite might enhance tellurite elimination and, hence, lead to higher yields of TeNPs production (Turner et al., 1994, 2012; Zannoni et al., 2008). As mentioned above, *Aromatoleum* sp. CIB displays moderate resistance to tellurite and needs more than 4 days to eliminate a significant amount of tellurite (Figure 2). Genome mining revealed that *Aromatoleum* sp. CIB lacks the well-characterized mechanisms of tellurite resistance encoded by the *ter*, *tehAB*, or *kilA* clusters (Chasteen et al., 2009; Taylor et al., 1994, 2002; Walter et al., 1991). However, the genome search has identified a *tpmt* gene (*AzCIB_0135*) whose product displays 40% amino acid sequence identity with the well-studied thiopurine *S*-methyltransferase (TPMT) from *P. syringae* that is able to methylate tellurite and increase bacterial resistance to this metalloid (Prigent-Combaret et al., 2012; Ranjard et al., 2002). A model of the tertiary structure of AzCIB_0135 predicted the conserved residues R123 and L55, responsible for substrate binding and enzymatic activation, respectively, as well as the surfaces involved in *S*-adenosylmethionine (SAM) recognition (Scheuermann et al., 2003; Figure S5). Therefore, we investigated whether *AzCIB_0135* could encode an ortholog of TPMT from *P. syringae* in *Aromatoleum* sp. CIB.

The *AzCIB_0135* gene was cloned and expressed under control of the *lacI*^{q}/*Ptac* regulatory couple that responds to the IPTG inducer in the broad-host range vector pIZ2, rendering plasmid pIZ2-0135 (Table 1). A synthetic *tpmt* gene that encodes a protein identical to TPMT from *P. syringae* (Figure S1) was also cloned in pIZ2 giving rise to plasmid pIZ2-TPMTPS (Table 1). Whereas *E. coli* DH10B (pIZ2) is able to tolerate a maximum concentration of <10 μM of tellurite, the strain *E. coli* DH10B (pIZ2-TPMTPS) increased its resistance up to 1 mM tellurite (Figure S6A) when IPTG was added to the cultures, which is in agreement with previous results showing that TPMT protein from *P. syringae* increased the tellurite resistance in *E. coli* MG1655 from 20 μM up to 1 mM (Prigent-Combaret et al., 2012). Interestingly, the strain *E. coli* DH10B (pIZ2-0135) that expresses the *AzCIB_0135* gene when IPTG is added to the cultures was able to grow in the presence of tellurite concentrations up to 3 mM (Figures S6A and S7B). Moreover, *E. coli* DH10B cells overproducing AzCIB_0135 in the presence of tellurite produced a strong garlic-like smell, which has been previously linked to the formation of methylated forms of the metalloid such as volatile dimethytelluride and dimethylditelluride (Prigent-Combaret et al., 2012; Ranjard et al., 2002). Therefore, all these results support the assumption that AzCIB_0135 from *Aromatoleum* sp. CIB is a methyltransferase involved in tellurite methylation, hence contributing to bacterial tellurite resistance.

Despite that described thiopurine *S*-methyltransferases involved in tellurite methylation were restricted so far to gamma-Proteobacteria (Prigent-Combaret et al., 2012), we have shown here that they are also present in *Aromatoleum* sp. CIB, a beta-Proteobacterium. We have also identified AzCIB_0135 orthologs in the genomes of other bacteria belonging to the *Azoarcus*/*Aromatoleum* group such as *Azoarcus* sp. Aa7 (93.8% identity, WP_191658506), *Aromatoleum toluolicum* (89.1% identity, WP_169143455), *Aromatoleum petrolei* (88.2% identity, WP_169207774), *Aromatoleum tolulyticum* (88.6% identity, WP_076602312), *Aromatoleum toluvorans* (81.4% identity, WP_169254381), *Azoarcus* sp. DN11 (79.2%, identity, WP_121426876), *Aromatoleum toluclasticus* (78.2% identity, WP_018988698), *Aromatoleum evansii* (78.6% identity, WP_169125277), *Azoarcus* sp. KH32C (62.1% identity, WP_015452291), *Aromatoleum diolicum* (66.35% identity, WP_169258614), *Azoarcus halotolerans* (61% identity, WP_159687877), and *Aromatoleum bremense* (67.3% identity, WP_169200935). Moreover, a search in the extensive number of bacterial genome sequences currently available in the databases revealed that these enzymes show a wider distribution

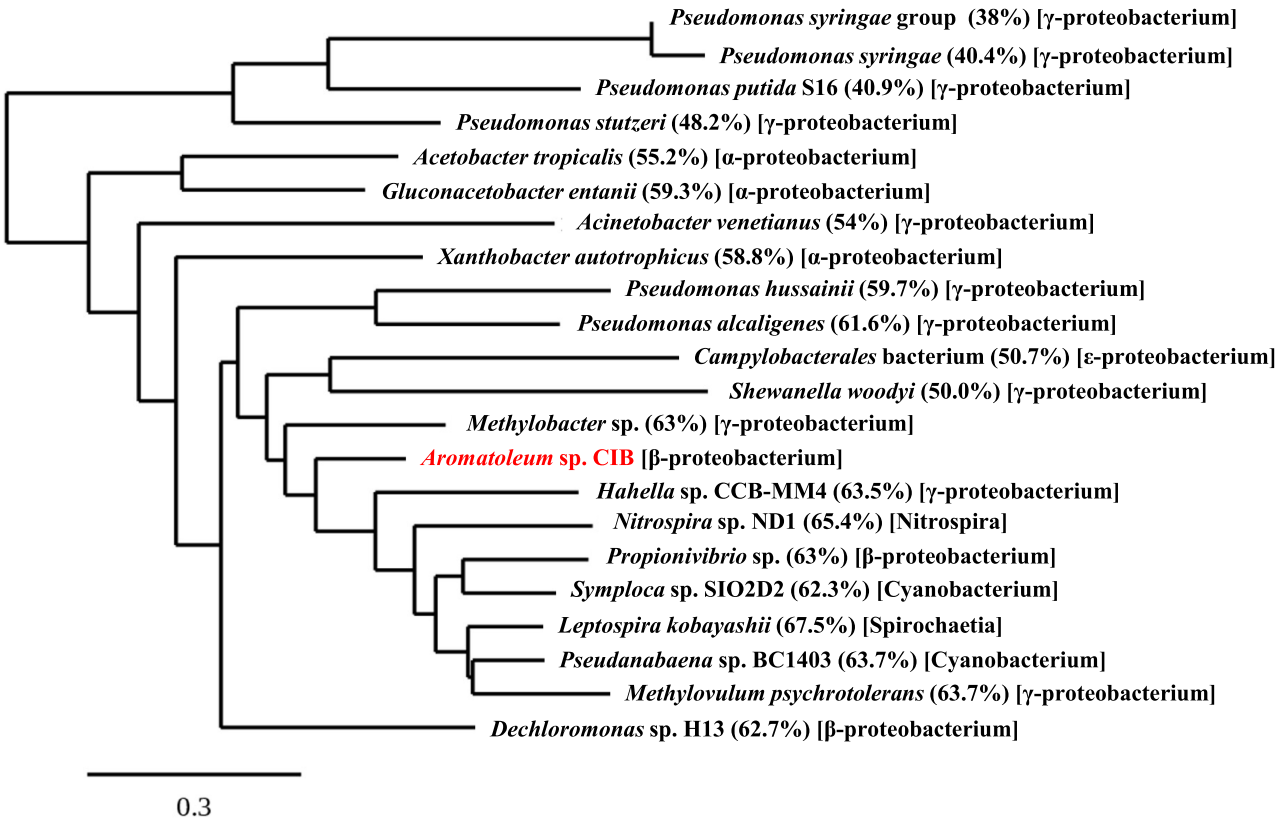

FIGURE 6 Phylogenetic tree of (putative) tellurite methyltransferase proteins. The clustering of each thiopurine methyltransferase to their taxonomical group is indicated. Proteins codes are: *Pseudomonas syringae* group (WP_003342681), *Pseudomonas syringae* (WP_122240818), *Pseudomonas stutzeri* (WP_041106389), *Pseudomonas putida* S16 (AEJ12082), *Acetobacter tropicalis* (WP_039904388), *Gluconacetobacter entanii* (WP_110913243), *Acinetobacter venetianus* (WP_061518019), *Xanthobacter autotrophicus* (WP_138397932), *Pseudomonas hussainii* (WP_074864070), *Pseudomonas alcaligenes* (WP_110682906), *Campylobacterales* bacterium (HHD75725), *Shewanella woodyi* (WP_065188016), *Methylobacter* sp. (PPC90099), *Aromatoleum* sp. CIB (WP_050414122), *Hahella* sp. CCB-MM4 (WP_094709600), *Nitrospira* sp. ND1 (WP_080877783), *Propionivibrio* sp. (MBK9029597), *Symploca* sp. SIO2D2 (NEQ69687), *Leptospira kobayashii* (WP_109022054), *Pseudanabaena* sp. BC1403 (WP_103669048), *Methylovulum psychrotolerans* (WP_088621629) and *Dechloromonas* sp. H13 (WP_153147638).

in the bacterial kingdom, being present also in beta-Proteobacteria other than *Aromatoleum*/*Azoarcus* group, in alpha- and epsilon-Proteobacteria, and in members of the Nitrospira, Spirochaetia and Cyanobacteria classes (Figure 6). Thus, these observations suggest that tellurite methylation can be more widespread than previously thought.

Enhancing tellurite resistance and TeNPs production by overexpressing AzCIB_0135 in *Aromatoleum* sp. CIB

Since the overexpression of *AzCIB_0135* increased tellurite resistance in *E. coli* cells, we checked whether its heterologous expression in the native host, i.e., *Aromatoleum* sp. CIB, could also lead to a recombinant strain with improved tellurite resistance. To this end, plasmid pIZ2-0135 was transferred to strain CIB, and we compared the anaerobic growth of the *Aromatoleum* sp. CIB (pIZ2) control strain with that of *Aromatoleum* sp. CIB (pIZ2-0135) in the presence of increasing concentrations of tellurite (Figure S8). It should be noted that the higher tellurite concentration that allowed growth of the *Aromatoleum* sp. CIB (pIZ2) control strain (0.2 mM; Figure S8) was slightly lower that that observed for the wild-type CIB strain (0.5 mM; Figure 1B), suggesting that the gentamicin needed for plasmid maintenance increases the cell stress with negative impact on tellurite resistance. Interestingly, when the *Aromatoleum* sp. CIB contained plasmid pIZ2-0135 expressing the IPTG-inducible *AzCIB_0135* gene, growth was observed up to 0.75 mM tellurite (Figure S8). Furthermore, the strain overproducing the AzCIB_0135 protein grew faster than the CIB strain in the presence of 0.1 mM tellurite (Figure 7A). All these results demonstrate that AzCIB_0135 protects from tellurite toxicity, thus leading to a higher resistance to this metalloid in *Aromatoleum* sp. CIB (pIZ2-0135).

We also explored the kinetics of tellurite elimination in *Aromatoleum* sp. CIB (pIZ2-0135) grown under

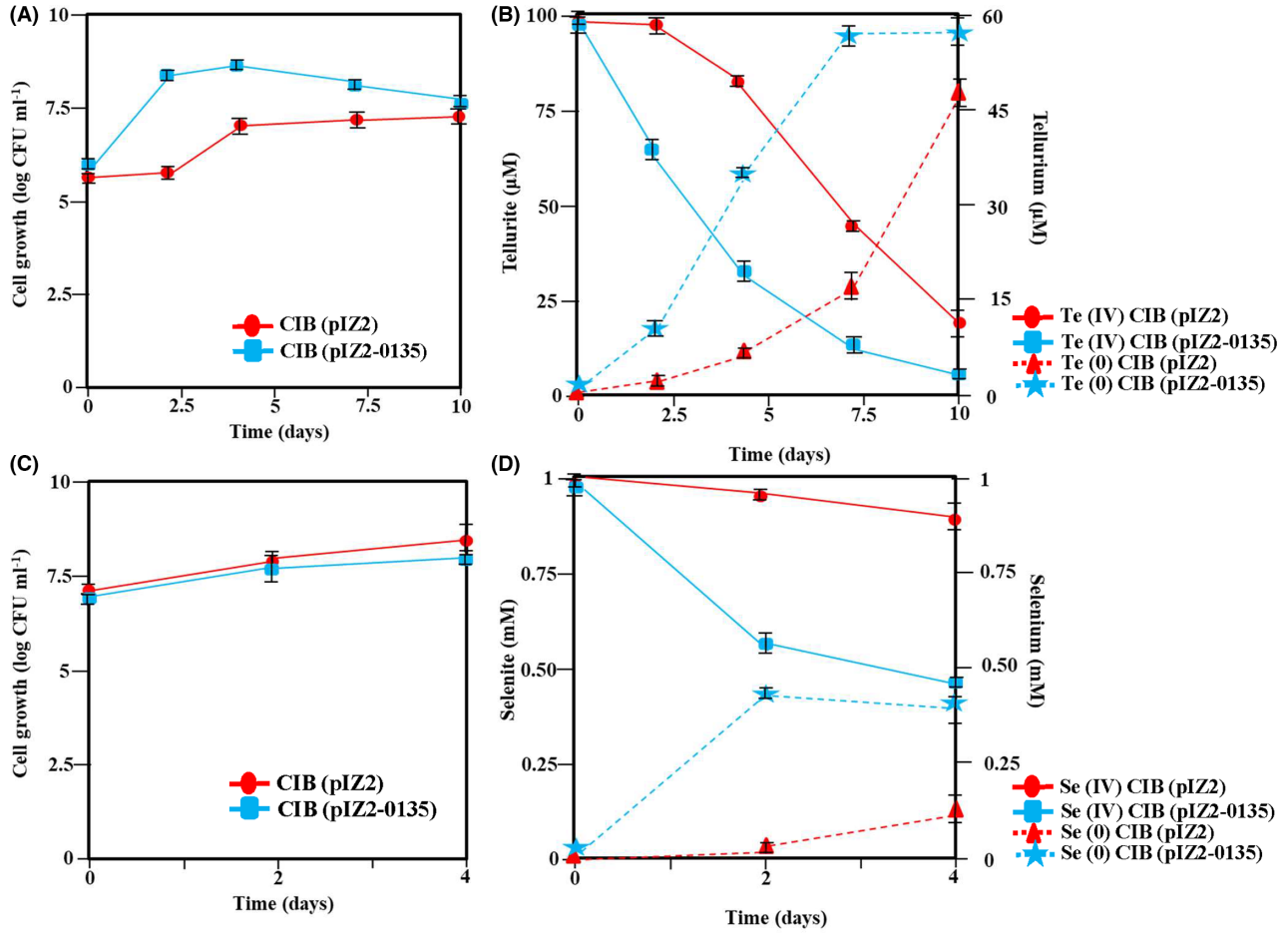

FIGURE 7 Time course of growth, tellurite, and selenite reduction, and Te (0) and Se (0) production by *Aromatoleum* sp. CIB (pIZ2) and *Aromatoleum* sp. CIB (pIZ2-0135) strains. (A) Kinetics of growth of CIB (pIZ2) cells (red) and CIB (pIZ2-0135) cells (blue). Cells were grown anaerobically in MC medium supplemented with 0.2% pyruvate, 0.5 mM IPTG and 0.1 mM tellurite, and the number of viable cells was measured as CFU ml^{-1}. (B) Tellurite depletion (continuous lines) and Te production (discontinuous lines) were determined by using ICP-OES as detailed in experimental procedures. (C) Kinetics of growth of CIB (pIZ2) cells (red) and CIB (pIZ2-0135) cells (blue). Cells were grown anaerobically in MC medium supplemented with 0.2% pyruvate, 0.5 mM IPTG and containing 1 mM selenite, and the number of cells was measured as CFU ml^{-1}. (D) Selenite depletion (continuous lines) and Se production (discontinuous lines) were determined by ICP-OES as detailed in experimental procedures. Error bars represent standard deviation of the values of at least three independent experiments.

anoxic conditions. Whereas the wild-type strain eliminates only 25% of tellurite after 5 days, the CIB strain overproducing AzCIB_0135 was able to remove around 75% of tellurite present in the medium, reaching values of 95% removal after 10 days of growth (Figure 7B). Therefore, the overproduction of AzCIB_0135 in strain CIB speeds-up tellurite removal, hence suggesting that the design of bacterial catalysts overexpressing a tellurite methylase constitutes a rational strategy to enhance tellurite elimination from environmental samples.

As indicated above, *E. coli* cells overproducing AzCIB_0135 increased tellurite resistance by more than 2 orders of magnitude, and a black colour corresponding to Te (0) deposits was observed in the bacterial cultures (Figure S6A). Similarly, cultures of *Aromatoleum* sp. CIB overproducing AzCIB_0135 also showed increased tellurite resistance and produced deposits darker than those of the wild type strain (Figure S6B). The analysis of the black deposits by TEM showed rod-shaped TeNPs of sizes compatible with those observed previously in the CIB strain (Figure S8A). The elemental analysis using EDX showed the electron-dense particles with specific Te absorption peaks (Figure 8B). The SAED pattern suggested that Te was also present in its crystalline form (Figure 8B, inset), which corresponds with crystallinity that characterizes the TeNPs produced by *Aromatoleum* sp. CIB.

The kinetics of Te (0) production in the wild-type CIB strain and the CIB strain overproducing AzCIB_0135 was compared (Figure 7B). After 5 days of growth, the production of Te (0) is around six times higher in the CIB strain overproducing AzCIB_0135 (6 $\mu mol\,h^{-1}\,L^{-1}$) than in the CIB strain (35 $\mu mol\,h^{-1}\,L^{-1}$; Figure 7B), which suggests that the tellurite methylase speeds-up the production of Te (0), in agreement with the higher tellurite tolerance and enhanced growth of this recombinant strain (Figure 7A).

All these results taken together revealed that *AzCIB_0135* represents an interesting genetic tool to

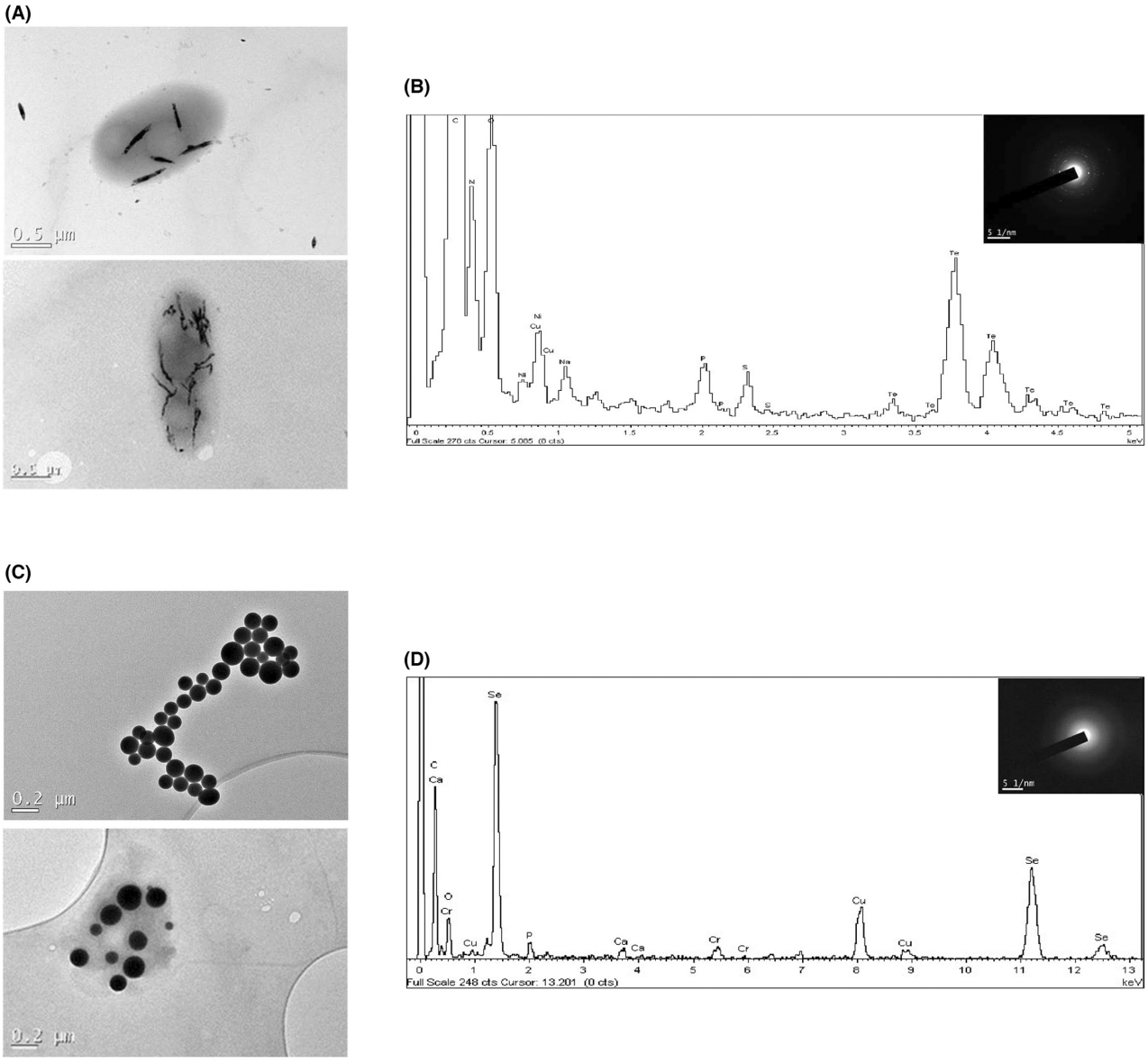

FIGURE 8 Electron microscopic observations of Te nanoparticles (TeNPs) and Se nanoparticles (SeNPs) produced by *Aromatoleum* sp. CIB (pIZ2-0135). (A) TeNPs were produced by cells grown anaerobically for 7 days in MC medium supplemented with 0.2% pyruvate, 0.5 mM IPTG and 0.1 mM tellurite (B) Energy-Dispersive X-ray spectroscopy (EDX) analysis of one TeNP. In the inset are shown the diffuse rings in the SAED (selected area electron diffraction) pattern of one TeNP. (C) SeNPs were produced by CIB (pIZ2-0135) cells grown anaerobically for 4 days in MC medium supplemented with 0.2 pyruvate, 0.5 mM IPTG, and 1 mM selenite. (D) EDX analysis of one SeNP. In the inset are shown the diffuse rings in the SAED (selected area electron diffraction) pattern of one SeNP.

increase bacterial resistance to tellurite, accelerating tellurite removal and the production of TeNPs in recombinant cells that overexpress this tellurite methylase.

The overexpression of AzCIB_0135 enhances also selenite elimination and Se nanoparticles (SeNPs) production in bacterial catalysts

It has been reported that *E. coli* cells expressing the *P. syringae* thiopurine methyltransferase (TPMT) also methylate selenite into dimethylselenide and dimethyldiselenide, which are 500–700 times less toxic than other derivatives (Ranjard et al., 2002, 2003). Moreover, it has been reported that Se biomethylation leads to detoxification and removal of Se from contaminated sites (Ranjard et al., 2003). Accordingly, *E. coli* DH10B (pIZ2-0135) strain overproducing AzCIB_0135 protein was able to tolerate higher concentrations of selenite (20 mM) than the DH10B (pIZ2) (10 mM) control strain (Figures S7C,D and S9A), and an orange colour appeared in the culture medium in the presence of selenite indicating the biological reduction from selenite to Se. In addition, a strong garlic smell appeared in the culture of DH10B overproducing AzCIB_0135

when selenite was present in the medium, suggesting the production of methylated selenite derivatives. These results show that AzCIB_0135 was able to protect the DH10B cells from the selenite toxicity most probably through the production of (methyl)selenides.

Previous results obtained in our laboratory demonstrated that *Aromatoleum* sp. CIB tolerates up to 5 mM selenite in anaerobic conditions (Fernández-Llamosas et al., 2016). Here, we show that the CIB strain harbouring the pIZ2 plasmid was not able to tolerate selenite concentrations higher than 2.5 mM (Figure S9B) suggesting that the gentamicin used to maintain the plasmid enhanced the stress produced by the metalloid. In any case, the overproduction of the AzCIB_0135 protein also increased moderately the tolerance of the strain to selenite (up to 5 mM, Figure S9B), although this recombinant strain did not grow faster than the wild-type strain in the presence of 1 mM selenite (Figure 7C).

Despite the overproduction of the AzCIB_0135 protein did not increase significantly the resistance to selenite, when we analysed the kinetics of selenite removal it was observed that whereas the wild-type strain eliminated only 15% selenite in 4 days of growth, the CIB strain overproducing AzCIB_0135 removed around 55% selenite after 4 days of cell growth (Figure 7D), and the kinetics of selenite elimination was significantly faster in the recombinant strain overexpressing *AzCIB_0135* (Figure 7D). Therefore, recombinant strains overexexpressing *AzCIB_0135* might be of biotechnological interest to eliminate selenite from environmental samples. In natural environments, the transformation of selenite to Se is linked to the decrease of toxicity, for example, the formation of the less toxic and mobile elemental Se from the reduction of selenite has importance in aquatic systems (Pettine et al., 2013). Moreover, orange deposits were clearly observed in cells overexpressing *AzCIB_0135* (Figure S9B), suggesting that a significant amount of selenite was reduced to Se (0). When the orange deposits were analysed by TEM, spherical SeNPs of around 100 nm diameter were observed (Figure 8C), and elemental analysis using EDX showed that the electron-dense particles presented the specific Se absorption peak (Figure 8D). The diffuse ring in the SAED pattern suggested that Se is present in its amorphous form (Figure 8D, inset), which corresponds to the size, morphology, and crystallinity that characterizes the SeNPs produced by *Aromatoleum* sp. CIB (Fernández-Llamosas et al., 2016). Interestingly, the overproduction of AzCIB_0135 caused a significant increase in the amount of Se (0) produced by the recombinant CIB cells, reaching about 50% of the selenite added to the culture medium after 2 days of growth (7.3 $\mu mol\, h^{-1}\, L^{-1}$), which contrasts with the almost no Se (0) production by the wild-type CIB cells at the same incubation time (0.1 $\mu mol\, h^{-1}\, L^{-1}$; Figure 7D).

In summary, all these results revealed that overproduction AzCIB_0135 constitutes a feasible genetic strategy to accelerate selenite elimination and the production of SeNPs in the recombinant bacterial cells. The increase of production of crystalline Te/Se in strains overproducing TPMT seems contradictory, since TPMT should increase the methylated forms and thus, decrease the amount of tellurite susceptible to be transformed in NPs. Nevertheless, it has been observed that in highly resistant bacteria able to methylate tellurite, still is possible to detect the production of significant amounts of Te as a product of their metabolism (Ollivier et al., 2011). A possible explanation might reside in the synergistic role of TPMT and reductases that participate in Te/Se production (Molina-Quiroz et al., 2014) in the decrease of stress produced by metalloids. As a consequence of this synergistic effect, an increased metalloid resistance is observed leading to higher rates of cell growth and, hence, to higher amounts of Te/Se accumulated. In any case, this apparent paradox needs to be solved experimentally.

CONCLUSIONS

The overexpression of molecular determinants responsible of metal and metalloid resistance was known to increase bacterial tolerance to such metal/metalloids and, in some cases, to enhance removal of such pollutans by their transformation into added value products such as metallic nanoparticles (Choi et al., 2018; Edmundson & Horsfall, 2015). Here, we have reported a new methyltransferase, the AzCIB_0135 protein from *Aromatoleum* sp. CIB, responsible for tellurite/selenite methylation. For the first time, we have shown that the overexpression of a methyltransferase speeds up the elimination of tellurite and selenite and enhances the production of TeNPs and SeNPs, respectively, which are both of high industrial interest. The fact that strain CIB also colonizes rice as an endophyte (Fernández-Llamosas et al., 2014) opens the prospect to use this microorganism to promote rice cultivation on metalloid contaminated soils.

AUTHOR CONTRIBUTIONS

Elena Alonso-Fernandes: Conceptualization (equal); formal analysis (equal); investigation (equal); methodology (equal). **Helga Fernández-Llamosas:** Conceptualization (equal); formal analysis (equal); investigation (equal); methodology (equal). **Irene Cano:** Investigation (equal); methodology (equal). **Cristina Serrano-Pelejero:** Investigation (equal); methodology (equal). **Laura Castro:** Conceptualization (equal); formal analysis (equal); investigation (equal); methodology (equal). **Eduardo Díaz:** Conceptualization (equal); funding acquisition (equal); resources (equal); supervision (equal); writing – review and editing (equal).

Manuel Carmona: Conceptualization (equal); funding acquisition (equal); methodology (equal); supervision (equal); writing – original draft (equal); writing – review and editing (equal).

ACKNOWLEDGMENTS

We thank A. Valencia for technical assistance and Secugen S.L. for DNA sequencing. This work was supported by grants BIO2016-79736-R, PID2019-110612RB-I00, PCI2019-111833-2 from the Ministry of Science and Innovation of Spain; by grant CSIC 2019 20E005, and by European Union H2020 Grant 101000733. Elena Alonso Fernandes and Cristina Serrano Pelejero wish to thank to the Spanish Ministry of Universities for the FPU17/02630 and FPU 20/05209 fellowships, respectively.

CONFLICT OF INTEREST

There are no conflicts of interest to declare.

ORCID

Manuel Carmona https://orcid.org/0000-0002-1591-7618

REFERENCES

Acedos, M.G., Torre, I., Santos, V.E., Garcia-Ochoa, F., García, J.L. & Galán, B. (2021) Modulating redox metabolism to improve isobutanol production in *Shimwellia blattae*. *Biotechnology for Biofuels*, 14, 8.

Avazéri, C., Turner, R.J., Pommier, J., Weiner, J.H., Giordano, G. & Verméglio, A. (1997) Tellurite reductase activity of nitrate reductase is responsible for the basal resistance of *Escherichia coli* to tellurite. *Microbiology*, 143, 1181–1189.

Ba, L.A., Doring, M., Jamier, V. & Jacob, C. (2010) Tellurium: an element with great biological potency and potential. *Organic & Biomolecular Chemistry*, 8, 4203–4216.

Baesman, S.M., Bullen, T.D., Dewald, J., Zhang, D., Curran, S., Islam, F.S. et al. (2007) Formation of tellurium nanocrystals during anaerobic growth of bacteria that use Te oxyanions as respiratory electron acceptors. *Applied and Environmental Microbiology*, 73, 2135–2143.

Baesman, S.M., Soltz, J.F., Kulo, T.R. & Oremland, R.S. (2009) Enrichment and isolation of *Bacillus beveridgei* sp. nov., a facultative anaerobic haloalkaliphile from mono Lake, California, that respires oxyanions of tellurium, selenium, and arsenic. *Extremophiles*, 13, 695–705.

Bahrami, K., Nazari, P., Sepehrizadeh, Z., Zarea, B. & Shahverdi, A.R. (2012) Microbial synthesis of antimony sulfide nanoparticles and their characterization. *Annals of Microbiology*, 62, 1419–1425.

Basaglia, M., Toffanin, A., Baldan, E., Bottegal, M., Shapleigh, J.P. & Casella, S. (2007) Selenite-reducing capacity of the copper-containing nitrite reductase of *Rhizobium sullae*. *FEMS Microbiology Letters*, 269, 124–130.

Blázquez, B., Carmona, M. & Díaz, E. (2018) Transcriptional regulation of the peripheral pathway for the anaerobic catabolism of toluene and *m*-xylene in *Azoarcus* sp. CIB. *Frontiers in Microbiology*, 9, 506.

Bonificio, W.D. & Clarke, D.R. (2014) Bacterial recovery and recycling of tellurium from tellurium-containing compounds by *Pseudoalteromonas* sp. EPR3. *Journal of Applied Microbiology*, 117, 1293–1304.

Borghese, R., Borsetti, F., Foladori, P., Ziglio, G. & Zannoni, D. (2004) Effect of the metalloid oxyanion tellurite (TeO_3^{2-}) on growth characteristics of the phototrophic bacterium *Rhodobacter capsulatus*. *Applied and Environmental Microbiology*, 70, 6595–6602.

Borghese, R., Brucale, M., Fortunato, G., Lanzi, M., Mezzi, A., Valle, F. et al. (2016) Extracellular production of tellurium nanoparticles by the photosynthetic bacterium *Rhodobacter capsulatus*. *Journal of Hazardous Materials*, 309, 202–209.

Borsetti, F., Tremaroli, V., Michelacci, F., Borghese, R., Winterstein, C., Daldal, R. et al. (2005) Tellurite effects on *Rhodobacter capsulatus* cell viability and superoxide dismutase activity under oxidative stress conditions. *Research in Microbiology*, 156, 807–813.

Bulgarini, A., Lampis, S., Turner, R.J. & Vallini, G. (2021) Biomolecular composition of capping-layer and stability of biogenic selenium nanoparticles synthesized by both gram positive and gram negative. *Microbial Biotechnology*, 14, 198–212.

Butler, C.S., Debieux, C.M., Dridge, E.J., Splatt, P. & Wright, M. (2012) Biomineralization of selenium by the selenate-respiring bacterium *Thauera selenatis*. *Biochemical Society Transactions*, 40, 1239–1243.

Calderón, I.L., Arenas, F.A., Pérez, J.M., Fuentes, D.E., Araya, M.A., Saavedra, C.P. et al. (2006) Catalases are NAD(P)H-dependent tellurite reductases. *PLoS One*, 1, e70.

Carmona, M., Zamarro, M.T., Blázquez, B., Durante-Rodríguez, G., Juárez, J.F., Valderama, J.A. et al. (2009) Anaerobic catabolism of aromatic compounds a genetic and genomic view. *Microbiology and Molecular Biology Reviews*, 73, 71–133.

Casadaban, M.J. & Cohen, S.N. (1980) Analysis of gene control signals by DNA fusion and cloning in *Escherichia coli*. *Journal of Molecular Biology*, 138, 179–207.

Chasteen, T.G., Fuentes, D.E., Tantaleán, J.C. & Vásquez, C.C. (2009) Tellurite: history, oxidative stress, and molecular mechanisms of resistance. *FEMS Microbiology Reviews*, 33, 820–832.

Chen, J. & Strous, M. (2013) Denitrification and aerobic respiration, hybrid electron transport chains and co-evolution. *Biochimica et Biophysica Acta*, 1827, 136–144.

Choi, Y., Park, T.J., Lee, D.C. & Lee, S.Y. (2018) Recombinant *Escherichia coli* as a biofactory for various single- and multi-element nanomaterials. *Proceedings of the National Academy of Sciences of the United States of America*, 115, 5944–5949.

Chou, T.M., Ke, Y.Y., Tsao, Y.H., Li, Y.C. & Lin, Z.H. (2016) Fabrication of Te and Te-Au nanowires-based carbon fiber fabrics for antibacterial applications. *International Journal of Environmental Research and Public Health*, 13, 202.

Collins, T.J. (2007) ImageJ for microscopy. *BioTechniques*, 43(1 Suppl), 25–30.

De Lorenzo, V. & Timmis, K.N. (1994) Analysis and construction of stable phenotypes in gram-negative bacteria with Tn*5*- and Tn*10*-derived minitransposons. *Methods in Enzymology*, 235, 386–405.

Debieux, C.M., Dridge, E.J., Mueller, C.M., Splatt, P., Paszkiewicz, K., Knight, I. et al. (2011) A bacterial process for selenium nanosphere assembly. *Proceedings of the National Academy of Sciences of the United States of America*, 108, 13480–13485.

Díaz-Vásquez, W.A., Abarca-Lagunas, M.J., Arenas, F.A., Pinto, C.A., Cornejo, F.A., Wansapura, P.T. et al. (2014) Tellurite reduction by *Escherichia coli* NDH-II dehydrogenase results in superoxide production in membranes of toxicant-exposed cells. *Biometals*, 27, 237–246.

Durante-Rodríguez, G., Fernández-Llamosas, H., Alonso-Fernandes, E., Fernández-Muñiz, M.N., Muñoz-Olivas, R., Díaz, E. et al. (2019) ArxA from *Azoarcus* sp. CIB, an anaerobic arsenite oxidase from an obligate heterotrophic and mesophilic bacterium. *Frontiers in Microbiology*, 10, 1699.

Edmundson, M.C. & Horsfall, L. (2015) Construction of a modular arsenic-resistance operon in *E. coli* and the production of arsenic nanoparticles. *Frontiers in Bioengineering and Biotechnology*, 3, 160.

Felsenstein, J. (1993) *PHYLIP (phylogenetic inference package) version 3.5.1*. Seattle, WA: University of Washington.

Fernández-Llamosas, H., Castro, L., Blázquez, M.L., Díaz, E. & Carmona, M. (2016) Biosynthesis of selenium nanoparticles by *Azoarcus* sp. CIB. *Microbial Cell Factories*, 15, 109.

Fernández-Llamosas, H., Castro, L., Blázquez, M.L., Díaz, E. & Carmona, M. (2017) Speeding up bioproduction of selenium nanoparticles by using *Vibrio natriegens* as microbial factory. *Scientific Reports*, 7, 16046.

Fernández-Llamosas, H., Ibero, J., Thijs, S., Imperato, V., Vangronsveld, J., Díaz, E. et al. (2020) Enhancing the rice seedlings growth promotion abilities of *Azoarcus* sp. CIB by heterologous expression of ACC deaminase to improve performance of plants exposed to cadmium stress. *Microorganisms*, 8, 1453.

Fernández-Llamosas, H., Prandoni, N., Fernández-Pascual, M., Fajardo, S., Morcillo, C., Díaz, E. et al. (2014) *Azoarcus* sp. CIB, an anaerobic biodegrader of aromatic compounds shows an endophytic lifestyle. *PLoS One*, 9, e110771.

Forootanfar, H., Amirpour-Rostami, S., Jafari, M., Forootanfar, A., Yousefizadeh, Z. & Shakibaie, M. (2015) Microbial-assisted synthesis and evaluation the cytotoxic effect of tellurium nanorods. *Materials Science and Engineering*, C49, 183–189.

Harrison, J.J., Ceri, H., Stremick, C. & Turner, R.J. (2004) Differences in biofilm and planktonic cell mediated reduction of metalloid oxyanions. *FEMS Microbiology Letters*, 235, 357–362.

Honchel, R., Aksoy, I.A., Szumlanski, C., Wood, T.C., Otterness, D.M., Wieben, E.D. et al. (1993) Human thiopurine methyltransferase: molecular cloning and expression of T84 colon carcinoma cell cDNA. *Molecular Pharmacology*, 43, 878–887.

Johnson, J.A., Saboungi, M.L., Thiyagarajan, P., Csencsits, R. & Meisel, D. (1999) Selenium nanoparticles: a small-angle neutron scattering study. *The Journal of Physical Chemistry. B*, 103, 59–63.

Juárez, J.F., Zamarro, M.T., Eberlein, C., Boll, M., Carmona, M. & Díaz, E. (2013) Characterization of the *mbd* cluster encoding the anaerobic 3-methylbenzoyl-CoA central pathway. *Environmental Microbiology*, 15, 148–166.

Jumper, J., Evans, R., Pritzel, A., Green, T., Figurnov, M., Ronneberger, O. et al. (2021) Highly accurate protein structure prediction with AlphaFold. *Nature*, 596, 583–589.

Kessi, J. & Hanselmann, K.W. (2004) Similarities between the abiotic reduction of selenite with glutathione and the dissimilatory reaction mediated by *Rhodospirillum rubrum* and *Escherichia coli*. *The Journal of Biological Chemistry*, 279, 50662–50669.

Kessi, J., Turner, R.J. & Zannoni, D. (2022) Tellurite and selenite: how can these two oxyanions be chemically different yet to similar in the way they are transformed to their metal forms by bacteria. *Biological Research*, 55, 17.

Kim, B. & Park, B. (2012) Synthesis of self-aligned tellurium nanotubes by a sodium thiosulfate-assisted polyol method. *Electronic Materials Letters*, 8, 33–36.

Kimura, M. (1980) A simple method for estimating evolutionary rates of base substitutions through comparative studies of nucleotide sequences. *Journal of Molecular Evolution*, 16, 111–120.

Li, B., Liu, N., Li, Y., Jing, W., Fan, J., Li, D. et al. (2014) Reduction of selenite to red elemental selenium by *Rhodopseudomonas palustris* strain N. *PLoS One*, 9, e95955.

López-Barragán, M.J., Carmona, M., Zamarro, M.T., Thiele, M., Boll, M., Fuchs, G. et al. (2004) The *bzd* gene cluster, coding for anaerobic benzoate catabolism in *Azoarcus* sp. CIB. *Journal of Bacteriology*, 186, 5762–5774.

Martín-Moldes, Z., Zamarro, M.T., del Cerro, C., Valencia, A., Gómez, M.J., Arcas, A. et al. (2015) Whole-genome analysis of *Azoarcus* sp. strain CIB provides genetic insights to its different lifestyles and predictsnovel metabolic features. *Systematic and Applied Microbiology*, 38, 462–471.

Miller, J.H. (1972) *Experiments in molecular genetics*. Cold Spring Harbor, NY: Cold Spring Harbor Laboratory Press.

Molina-Quiroz, R.C., Loyola, D.E., Díaz-Vásquez, W.A., Arenas, F.A., Urzúa, U., Pérez-Donoso, J.M. et al. (2014) Global transcriptomic analysis uncovers a switch to anaerobic metabolism in tellurite-exposed *Escherichia coli*. *Research in Microbiology*, 165, 566–570.

Montenegro, R., Vieto, S., Wicki-Emmenegger, D., Vásquez-Castro, F., Coronado-Ruiz, C. Fuentes-Schweizer, P. et al. (2020) The putative phosphate transporter PitB (PP1373) is involved in tellurite uptake in *Pseudomonas putida* KT2440. *bioRxiv*. Available from: https://doi.org/10.1101/2020.08.24.265637

Moore, M. & Kaplan, S. (1992) Identification of intrinsic high-level resistance to rare-earth oxides and oxyanions in members of the class proteobacteria: characterization of tellurite, selelnote and rhodium sesquioxide reduction in *Rhodobacter sphaeroides*. *Journal of Bacteriology*, 134, 1505–1514.

Moreno-Martin, G., Sanz-Landaluze, J., León-González, M.E. & Madrid, Y. (2021) In vivo quantification of volatile organoselenium compounds released by bacteria exposed to selenium with HS-SPME-GC-MS effect of selenite and selenium nanoparticles. *Talanta*, 224, 121907.

Moreno-Ruiz, E., Hernáez, M.J., Martínez-Pérez, O. & Santero, E. (2003) Identification and functional characterization of *Sphingomonas macrogolitabida* strain TFA genes involved in the first two steps of the tetralin catabolic pathway. *Journal of Bacteriology*, 185, 2026–2030.

Morlon, H., Fortin, C., Floriani, M., Adam, C., Garnier-Laplace, J. & Boudou, A. (2005) Toxicity of selenite in the unicellular green alga *Chlamydomonas reinhardtii*: comparison between effects at the population and sub-cellular level. *Aquatic Toxicology*, 73, 65–78.

Muñoz-Díaz, P., Jiménez, K., Luraschi, R., Cornejo, F., Figueroa, M., Vera, C. et al. (2022) Anaerobic RSH-dependent tellurite reduction contributes to *Escherichia coli* tolerance against tellurite. *Biological Research*, 55, 13.

Nawaz, F., Ahmad, R., Ashraf, M.Y., Waraich, E.A. & Khan, S.Z. (2015) Effect of selenium foliar spray on physiological and biochemical processes and chemical constituents of wheat under drought stress. *Ecotoxicology and Environmental Safety*, 113, 191–200.

Nguyen, V.K., Choi, W., Ha, Y., Gu, Y., Lee, C., Park, J. et al. (2019) Microbial tellurite reduction and production of elemental tellurium nanoparticles by novel bacteria isolated from wastewater. *Journal of Industrial and Engineering Chemistry*, 78, 246–256.

Ollivier, P.R.L., Bahrou, A.S., Church, T.M. & Hanson, T.E. (2011) Aeration controls the reduction and methylation of tellurium by the aerobic, tellurite-resistant marine yeast *Rhodotorula mucilaginosa*. *Applied and Environmental Microbiology*, 77, 4610–4617.

Pérez, J.M., Calderón, I.L., Arenas, F.A., Fuentes, D.E., Pradenas, G.A., Fuentes, E.L. et al. (2007) Bacterial toxicity of potassium tellurite: unraveling an ancient enigma. *PLoS One*, 2, e211.

Pettine, M., Gennari, F. & Campanella, L. (2013) The reaction of selenium (IV) with ascorbic acid: its relevance in aqueous and soil systems. *Chemosphere*, 90, 245–250.

Piacenza, E., Presentato, A. & Turner, R.J. (2018) Stability of biogenic metal(loid) nanomaterial related to the colloidal stabilization theory of chemical nanostructures. *Critical Reviews in Biotechnology*, 38, 1137–1156.

Piacenza, E., Presentato, A., Zonaro, E., Lampis, S., Vallini, G. & Turner, R.J. (2018) Selenium and tellurium nanomaterials. *Physical Sciences Reviews*, 3, 20170100.

Presentato, A., Piacenza, E., Darbandi, A., Anikovskiy, M., Cappelletti, M., Zannoni, D. et al. (2018) Assembly, growth

and conductive properties of tellurium nanorods produced by *Rhodococcus aetherivorans* BCP1. *Scientific Reports*, 8, 3923.

Presentato, A., Turner, R.J., Vázques, C.C., Yurkov, V. & Zannoni, D. (2019) Tellurite-dependent blackening of bacteria emerges from the dark ages. *Environment and Chemistry*, 16, 266–288.

Prigent-Combaret, C., Sanguin, H., Champier, L., Bertrand, C., Monnez, C., Colinon, C. et al. (2012) The bacterial thiopurine methyltransferase tellurite resistance process is highly dependent upon aggregation properties and oxidative stress response. *Environmental Microbiology*, 14, 2645–2660.

Ramos-Ruiz, A., Field, J.A., Wilkening, J.V. & Sierra-Alvarez, R. (2016) Recovery of elemental tellurium nanoparticles by the reduction of tellurium oxyanions in a methanogenic microbial consortium. *Environmental Science & Technology*, 50, 1492–1500.

Ranjard, L., Nazaret, S. & Cournoyer, B. (2003) Freshwater bacteria can methylate selenium through the thiopurine methyltransferase pathway. *Applied and Environmental Microbiology*, 69, 3784–3790.

Ranjard, L., Prigent-Combaret, C., Nazaret, S. & Cournoyer, B. (2002) Methylation of inorganic and organic selenium by the bacterial thiopurine methyltransferase. *Journal of Bacteriology*, 184, 3146–3149.

Roy, S. & Hardej, D. (2011) Tellurium tetrachloride and diphenyl ditelluride cause cytotoxicity in rat hippocampal astrocytes. *Food and Chemical Toxicology*, 49, 2564–2574.

Ruiz-Fresneda, M.A., Eswayah, A.S., Romero-González, M.R., Gardiner, P.H.E., Solari, P.L. & Merroun, M.L. (2020) Chemical and structural characterization of Se IV biotransformations by *Stenotrophomonas bentonitica* into se^0 nanostructures and volatiles Se species. *Environmental Science. Nano*, 7, 2140–2155.

Sabaty, M., Avazeri, C., Pignol, D., Adriano, J.M. & Vermeglio, A. (2001) Characterization of the reduction of selenate and tellurite by nitrate reductases. *Applied and Environmental Microbiology*, 67, 5122–5126.

Saitou, N. & Nei, M. (1987) The neighbor-joining method: a new method for reconstructing phylogenetic trees. *Molecular Biology and Evolution*, 4, 406–425.

Sambrook, J. & Rusell, D. (2001) *Molecular cloning: a laboratory manual*. New York, NY: Cold Spring Harbor Laboratory Press.

Sanger, F., Nicklen, S. & Coulson, A.R. (1977) DNA sequencing with chain-termining inhibitors. *Proceedings of the National Academy of Sciences of the United States of America*, 74, 5463–5467.

Scheuermann, T.H., Lolis, E. & Hodsdon, M.E. (2003) Tertiary structure of thiopurine methyltransferase from *Pseudomonas syringae*, a bacterial orthologue of a polymorphic, drug-metabolizing enzyme. *Journal of Molecular Biology*, 333, 573–585.

Shie, M.D. & Deeds, F.E. (1920) The importance of tellurium as a health hazard in industry. A preliminary report. *Public Health Reports*, 35, 939–954.

Summers, A.O. & Jacoby, G.A. (1977) Plasmid-determined resistance to tellurium compounds. *Journal of Bacteriology*, 129, 276–281.

Tantaleán, J.C., Araya, M.A., Saavedra, C.P., Fuentes, D.E., Pérez, J.M., Calderón, I.L. et al. (2003) The *Geobacillus stearothermophilus* V *iscS* gene, encoding cysteine desulfurase, confers resistance to potassium tellurite in *Escherichia coli* K-12. *Journal of Bacteriology*, 185, 5831–5837.

Taylor, A. (1996) Biochemistry of tellurium. *Biological Trace Element Research*, 55, 231–239.

Taylor, D. (1999) Bacterial tellurite resistance. *Trends in Microbiology*, 7, 111–115.

Taylor, D.E., Hou, Y., Turner, R.J. & Weiner, J.H. (1994) Location of a potassium tellurite resistance operon (*tehA tehB*) within the terminus of *Escherichia coli* K-12. *Journal of Bacteriology*, 176, 2740–2742.

Taylor, D.E., Rooker, M., Keelan, M., Ng, L.-K., Martin, I., Perna, N.T. et al. (2002) Genomic variability of O islands encoding tellurite resistance in enterohemorrhagic *Escherichia coli* O157:H7 isolates. *Journal of Bacteriology*, 184, 4690–4698.

Thakkar, K.N., Mhatre, S.S. & Parikh, R.Y. (2010) Biological synthesis of metallic nanoparticles. *Nanomedicine: Nanotechnology, Biology and Medicine*, 6, 257–262.

Thompson, J.D., Higgins, D.G. & Gibson, T.J. (1994) CLUSTAL W: improving the sensitivity of progressive multiple sequence alignment through sequence weighting, position-specific gap penalties and weight matrix choice. *Nucleic Acids Research*, 22, 4673–4680.

Tremaroli, V., Fedi, S. & Zannoni, D. (2007) Evidence for a tellurite-dependent generation of reactive oxygen species and absence of a tellurite-mediated adaptive response to oxidative stress in cells of *Pseudomonas pseudoalcaligenes* K707. *Archives of Microbiology*, 187, 127–135.

Trutko, S.M., Akimenko, V.K., Suzina, N.E., Anisimova, L.A., Shlyapnikov, M.G., Baskunov, B.P. et al. (2000) Involvement of the respiratory chain of gram-negative bacteria in the reduction of tellurite. *Archives of Microbiology*, 173, 178–186.

Tucker, F.L., Walper, J.E., Appleman, M.D. & Donohue, J. (1962) Complete reduction of tellurite to pure tellurium metal by microorganisms. *Journal of Bacteriology*, 83, 1313–1314.

Turner, R.J., Borghese, R. & Zannoni, D. (2012) Microbial processing of tellurium as a tool in biotechnology. *Biotechnology Advances*, 30, 954–963.

Turner, R.J., Weiner, J.H. & Taylor, D.E. (1994) Utility of plasmid borne tellurite resistance determinants for the bio-recovery of tellurium. *Biorecovery*, 2, 221–225.

Turner, R.J., Weiner, J.H. & Taylor, D.E. (1998) Selenium metabolism in *Escherichia coli*. *Biometals*, 11, 223–227.

Valdivia-González, M.A., Díaz-Vásquez, W.A., Ruiz-León, D., Becerra, A.A., Aguayo, D.R., Pérez-Donoso, J.M. et al. (2018) A comparative analysis of tellurite detoxification by members of the genus *Shewanella*. *Archives of Microbiology*, 200, 267–273.

Vij, P. & Hardej, D. (2012) Evaluation of tellurium toxicity in transformed and non-transformed human colon cells. *Environmental Toxicology and Pharmacology*, 34, 768–782.

Walter, E.G., Thomas, C.M., Ibbotson, J.P. & Taylor, D.E. (1991) Transcriptional analysis, translational analysis, and sequence of the kilA-tellurite resistance region of plasmid RK2Ter. *Journal of Bacteriology*, 173, 1111–1119.

Widy-Tyszkiewicz, E., Piechal, A., Gajkowska, B. & Smialek, M. (2002) Tellurium induced cognitive deficits in rates are related to neuro-pathological changes in the central nervous system. *Toxicology Letters*, 131, 203–214.

Wiklund, J.A., Kirk, J.L., Muir, D.C.G., Carrier, J., Gleason, A., Yang, F. et al. (2018) Widespread atmospheric tellurium contamination in industrial and remote regions of Canada. *Environmental Science & Technology*, 52, 6137–6145.

Wu, X., Jinming, S. & Xuegang, L. (2014) Occurrence and distribution of dissolved tellurium in Changjiang River estuary. *Chinese Journal of Oceanology and Limnology*, 32, 444–454.

Xie, H.G., Xia, W., Chen, M., Wu, L.C. & Tong, J. (2018) Isolation and characterization of the tellurite-reducing photosynthetic bacterium, *Rhodopseudomonas palustris* strain TX618. *Water, Air, and Soil Pollution*, 229, 158.

Zannoni, D., Borsetti, F., Harrison, J.J. & Turner, R.J. (2008) The bacterial response to the chalcogen metalloids Se and Te. *Advances in Microbial Physiology*, 53, 1–72.

Zare, B., Faramarzi, M.A., Sepehrizadeh, Z., Shakibaie, M., Rezaie, S. & Shahverdi, A.R. (2012) Biosynthesis and recovery of rod-shaped tellurium nanoparticles and their bactericidal activities. *Materials Research Bulletin*, 47, 3719–3725.

Zonaro, E., Lampis, S., Turner, R.J., Qazi, S.J.S. & Vallini, G. (2015) Biogenic selenium and tellurium nanoparticles synthesized by environmental microbial isolates efficaciously inhibit bacterial planktonic cultures and biofilms. *Frontiers in Microbiology*, 6, 584.

SUPPORTING INFORMATION

Additional supporting information can be found online in the Supporting Information section at the end of this article.

How to cite this article: Alonso-Fernandes, E., Fernández-Llamosas, H., Cano, I., Serrano-Pelejero, C., Castro, L. & Díaz, E. et al. (2022) Enhancing tellurite and selenite bioconversions by overexpressing a methyltransferase from *Aromatoleum* sp. CIB. *Microbial Biotechnology*, 00, 1–16. Available from: https://doi.org/10.1111/1751-7915.14162